

**SIMULATED TORNADIC VORTEX AND REFLECTIVITY SIGNATURES  
OF NUMERICALLY MODELED TORNADOES HAVING WEAK ECHO HOLES**

Vincent T. Wood and Rodger A. Brown  
NOAA/OAR/National Severe Storms Laboratory, Norman, Oklahoma

**1. INTRODUCTION**

A tornadic vortex signature (TVS) is a degraded Doppler velocity signature that occurs when a tornado is smaller than the half-power beamwidth (angular difference between the half-power points) of a sampling Doppler radar. Early simulations, which used a uniform reflectivity distribution across an assumed-Rankine (Rankine 1882) tornado vortex, showed that the extreme Doppler velocity values were separated by about one beamwidth. Fig. 1 illustrates that even though the TVS associated with a given tornado decreases in magnitudes as the radar beam becomes broader, the peak values of the TVS remain essentially the same distance apart – about one beamwidth. Fig. 2 presents Doppler velocity measurements (dots) through the center of the Union City, OK tornado of 24 May 1973 using an NSSL research Doppler radar (Brown et al. 1978). The dots are superimposed on three theoretical TVS curves produced by scanning a simulated radar past three Rankine vortices having various sizes and strengths. Although Doppler velocity data points nicely fit the simulated TVS curves (Fig. 2), the TVS strength does not reveal the strength or size of the tornado itself.

For a scanning radar with a beamwidth of approximately  $1.0^\circ$  and data collected at  $1.0^\circ$  azimuthal intervals, the two extreme Doppler velocity measurements appear at adjacent azimuth locations, commonly called “gate-to-gate shear”, and occasionally are separated by  $2.0^\circ$  (every other azimuthal location when one azimuthal location is close to the center of the tornado; e.g., Wood and Brown 1997). However, with the recent beginning of  $0.5^\circ$  azimuthal sampling (“super resolution”) by WSR-88D radars, the extreme measurements occasionally appear at  $0.5^\circ$  (which is much less than one beamwidth) instead of  $1.0^\circ$  azimuthal intervals (Brown and Wood 2011). The question that needs to be addressed is: Why do the super-resolution Doppler velocity measurements disagree with the earlier simulations that assumed uniform reflectivity across the Rankine tornado? The purpose of this study is to answer this question by running new Doppler radar simulations using a more realistic vortex model (instead of the Rankine model) and a more representative reflectivity distribution having a weak-reflectivity eye across the vortex.

**2. DOPPLER RADAR EMULATOR**

For the Doppler radar computations, we used a

Doppler radar emulator that approximates the basic characteristics of a WSR-88D (Weather Surveillance Radar-1988 Doppler); see the appendix of Wood and Brown (1997) for details. When a radar antenna rotates during the time period that a representative number of samples are being collected, the beamwidth is effectively broadened (Doviak and Zmric 1993, pp. 193-197). When a WSR-88D collects data at  $1.0^\circ$  azimuthal *legacy* intervals, the beamwidth increases from  $0.9^\circ$  (the stationary antenna beamwidth) to an effective beamwidth of  $1.4^\circ$  (e.g., Brown et al. 2002). For  $0.5^\circ$  azimuthal *super-resolution* data collection, the effective beamwidth broadens to only  $1.0^\circ$ .

Following is an overview of assumptions made for the emulator. Instead of the radar beam consisting of a main lobe and side lobes, it consisted only of a main lobe that was represented by a Gaussian distribution. For simplicity, the radar scanned horizontally through the vortex only at the range of the vortex center from the radar. Furthermore, we assumed that the tangential velocity and reflectivity profiles across the vortex were constant with height, so that, instead of making the measurements throughout the two-dimensional (elevation-azimuth) beam, the measurements were made horizontally through the center of the beam. Emulating the full width of a WSR-88D beam, we assumed that the full effective beamwidth excluding the sidelobes was Gaussian shaped and equal to three times the half-power effective beamwidth, which is a very good approximation of the WSR-88D beam. Additionally, we assumed that the radar measurements were continuous and free of noise. Instead of averaging radar pulses to produce simulated mean Doppler velocity values, mean Doppler velocity values were computed by averaging distributed tangential velocity values across the effective beamwidth.

**3. DOPPLER RADAR SIMULATION RESULTS**

We investigate the effects of nonuniform reflectivity on the characteristics of the TVS and compare the results with the TVS characteristics associated with the uniform reflectivity region. We chose the Burgers-Rott (Burgers 1948; Rott 1958) vortex model to represent the tornado’s tangential velocity profile because the profile agrees favorably with Doppler velocity measurements made by mobile Doppler radars close to tornadoes (Bluestein et al. 2007; Tanamachi et al. 2007; Kosiba and Wurman 2010). The nonuniform reflectivity profile consisted of a weak-reflectivity eye at the center of the tornado. The profile was based on blending of several profiles computed from observed Doppler measurements (e.g., Wakimoto and Martner 1992; Wurman and Gill

---

*Corresponding author address:* Vincent T. Wood, National Severe Storms Laboratory, 120 David L. Boren, Blvd., Norman, OK 73072-7323. E-mail: Vincent.Wood@noaa.gov

2000; Wakimoto et al. 2011) and from the numerical model studies of Wood et al. (2009). The relationship between the Burgers-Rott tangential velocity profile and the weak-reflectivity-eye profile is illustrated in Fig. 3. The peak reflectivity occurs at twice the core radius at which the maximum tangential velocity occurs, indicative of the centrifuging of radar targets. This relationship resembles that observed in proximity mobile Doppler radar measurements (e.g., Wurman and Gill 2000; Bluestein 2005; Wakimoto et al. 2011).

The most obvious differences in the TVS diameters between the two different reflectivity profiles occur when the effective beamwidth is from 1.0 to approximately 2.5 times larger than the tornado's core diameter (Fig. 4). With the presence of a uniform reflectivity region, TVS diameters are 0.9 to 1.3 times the effective beamwidth, while for a reflectivity eye, TVS diameters are 0.7 to 0.8 times the effective beamwidth. When a WSR-88D collects super-resolution data at 0.5° azimuthal interval, the effective beamwidth is 1.0° (e.g., Brown et al. 2002). Therefore, peak TVS values are expected to be 0.7° to 0.8° apart with minimum reflectivity at the center of the tornado. This means that, with super-resolution data collection, the peak TVS values can be separated by either 0.5° (adjacent azimuthal locations) or 1.0° (every other azimuthal location).

When the radar's effective beamwidth is at least 2.5 times larger than the core diameter of the vortex, there are no significant TVS differences between the reflectivity profiles (Fig. 4). The distance between the extreme WSR-88D Doppler velocity values are equal to 0.8 to 0.9 times the effective beamwidth (Fig. 4). For both legacy-resolution with 1.0° azimuthal sampling interval (EBW = 1.4°) and super-resolution with 0.5° azimuthal sampling interval (EBW = 1.0°), the peaks are expected to be separated by 1.0°.

#### 4. CONCLUSIONS

Doppler radar simulation results indicate that, using two different reflectivity profiles in which the Burgers-Rott vortex is embedded, there was a significant difference in TVS diameter when the effective beamwidth was less than 2.5 times larger than the vortex's core diameter. With the presence of a reflectivity eye (due to centrifuged radar targets), it is possible for the distance between the peak Doppler velocity values to be separated by 0.5° for super-resolution data collection. However, when the effective beamwidth is greater than 2.5 times the core diameter, the peak values are expected to have an azimuthal separation of 1.0° for both legacy-resolution (one azimuthal increment) and super-resolution (two azimuthal increments) data collection.

#### 5. ACKNOWLEDGMENTS

We would like to thank Kevin Manross of NSSL for reading and making suggestions in this paper.

#### 6. REFERENCES

- Bluestein, H. B., 2005: A review of ground-based mobile, W-band Doppler-radar observations of tornadoes and dust devils. *Dyn. Atmos. Oceans*, **40**, 163-188.
- \_\_\_\_\_, C. C. Weiss, M. M. French, E. M. Holthaus, and R. L. Tanamachi, 2007: The structure of tornadoes near Attica, Kansas, on 12 May 2004: High-resolution, mobile, Doppler radar observations. *Mon. Wea. Rev.*, **135**, 475-506.
- Brown, R. A., and V. T. Wood, 2011: The tornadic vortex signature (TVS). Preprints, *39<sup>th</sup> Conf. on Broadcast Meteor.*, Oklahoma City, OK, Amer. Meteor. Soc., p. 8.
- \_\_\_\_\_, L. R. Lemon, and D. W. Burgess, 1978: Tornado detection by pulsed Doppler radar. *Mon. Wea. Rev.*, **106**, 29-38.
- \_\_\_\_\_, V. T. Wood, and D. Sirmans, 2002: Improved tornado detection using simulated and actual WSR-88D data with enhanced resolution. *J. Atmos. Oceanic Technol.*, **19**, 1759-1771.
- Burgers, J. M., 1948: A mathematical model illustrating the theory of turbulence. *Adv. Appl. Mech.*, **1**, 171-199.
- Doviak, R. J., and D. S. Zrnić, 1993: *Doppler Radar and Weather Observations*. 2<sup>nd</sup> ed. Academic Press, 562 pp.
- Kosiba, K., and J. Wurman, 2010: The three-dimensional axisymmetric wind field structure of the Spencer, South Dakota, 1998 tornado. *J. Atmos. Sci.*, **67**, 3074-3083.
- Rankine, W. J. M., 1882: *A Manual of Applied Physics*. 10<sup>th</sup> ed., Charles Griff and Co., 663 pp.
- Rott, N., 1958: On the viscous core of a line vortex. *Z. Angew. Math. Phys.*, **9**, 543-553.
- Tanamachi, R. L., H. B. Bluestein, W.-C. Lee, M. Bell, and A. Pazmany, 2007: Ground-based velocity track display (GBVTD) analysis of W-band Doppler radar data in a tornado near Stockton, Kansas, on 15 May 1999. *Mon. Wea. Rev.*, **135**, 783-800.
- Wakimoto, R. M., and B. E. Martner, 1992: Observations of a Colorado tornado. Part II: Combined photogrammetric and Doppler radar analysis. *Mon. Wea. Rev.*, **120**, 522-543.
- \_\_\_\_\_, N. T. Atkins, and J. Wurman, 2011: The LaGrange tornado during VORTEX2. Part I: Photogrammetric analysis of the tornado combined with single-Doppler radar data. *Mon. Wea. Rev.*, **139**, 2233-2258.
- Wood, V. T., and R. A. Brown, 1997: Effects of radar sampling on single-Doppler velocity signatures of mesocyclones and tornadoes. *Wea. Forecasting*, **12**, 928-938.
- \_\_\_\_\_, \_\_\_\_\_, and D. C. Dowell, 2009: Simulated WSR-88D velocity and reflectivity signatures of numerically modeled tornadoes. *J. Atmos. Oceanic Technol.*, **26**, 876-893.
- Wurman, J., and S. Gill, 2000: Finescale radar observations of the Dimmitt, Texas (2 June 1995), tornado. *Mon. Wea. Rev.*, **128**, 2135-2164.

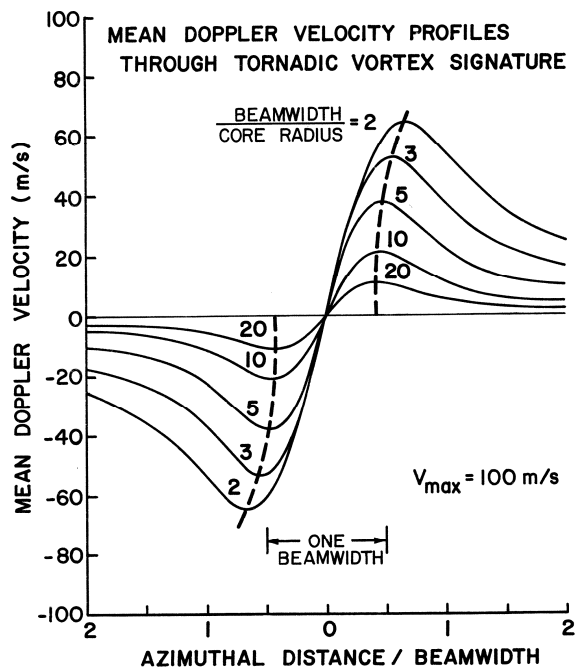


Fig. 1. Simulated azimuthal Doppler velocity profiles through the center of a tornadic vortex signature for various beamwidth to core radius ratios (representing various ranges from the radar for a given vortex). The abscissa is normalized by dividing the azimuthal distance from the vortex center by the radar's half-power beamwidth ( $0.8^\circ$ ). The maximum tangential velocity of the Rankine vortex is  $100 \text{ m s}^{-1}$ . The simulations assumed uniform reflectivity across the vortex. From Brown et al. (1978).

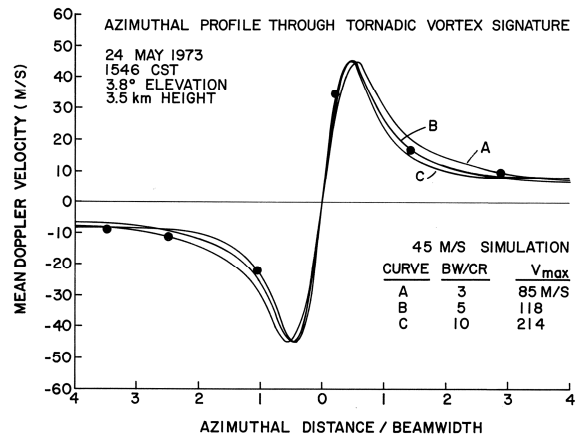


Fig. 2. Doppler velocity measurements (dots) through the center of the Union City, Oklahoma tornado superimposed on three theoretical TVS curves produced by scanning a simulated radar past three Rankine vortices having distinctly different sizes (ratio of beamwidth  $BW$  to core radius  $CR$ ) and peak tangential velocities ( $V_{max}$ ). Reflectivity across the vortices was assumed to be uniform. From Brown et al. (1978).

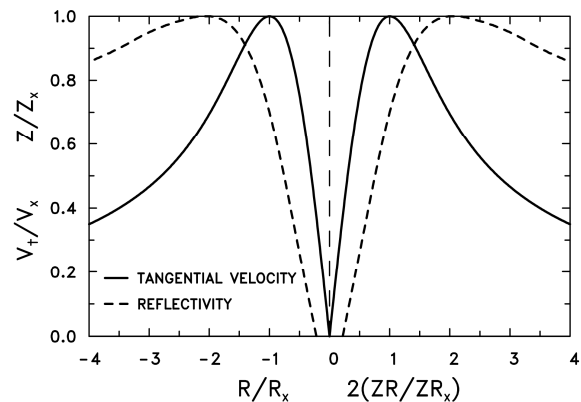


Fig. 3. Relationship of the normalized reflectivity profile (relative to the peak value  $Z_x$ ) to the normalized Burgers-Rott tangential velocity (relative to the peak value  $V_x$ ) as a function of radius ( $ZR, R$ ) from the vortex center normalized by the radius of the respective peak values ( $ZR_x, R_x$ );  $ZR$  is radius of the reflectivity profile and  $R$  is radius of the tangential velocity profile. Vertical dashed line is the vortex center.

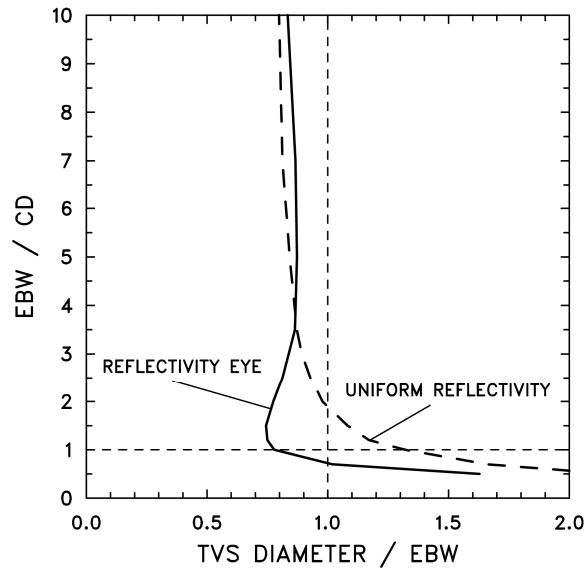


Fig. 4. Simulated TVS diameter relative to the effective beamwidth (EBW) for two reflectivity profiles (solid and long-dashed curves) across the Burgers-Rott vortex as a function of the ratio of the effective beamwidth to the true core diameter (CD) of the vortex. The Doppler velocity signature is defined as a TVS when the effective beamwidth is greater than the core diameter of the vortex (above the horizontal dashed line at  $EBW/CD = 1.0$ ).